Novel Metal-[Metal Oxide]-Nonmetal Sandwich-Like Superalkali Compounds Li3OMC5H5 (M = Be, Mg, and Ca): How to Increase the Aromaticity of Li-3(+) Ring?

ARTICLE *in* INTERNATIONAL JOURNAL OF QUANTUM CHEMISTRY · JANUARY 2009

Impact Factor: 1.43 · DOI: 10.1002/qua.22349

5 AUTHORS, INCLUDING:

Yin-Feng Wang
Jinggangshan University
20 PUBLICATIONS **177** CITATIONS
SEE PROFILE

Wei Chen
Kyoto University
167 PUBLICATIONS **1,898** CITATIONS
SEE PROFILE

Novel Metal-[Metal Oxide]-Nonmetal Sandwich-Like Superalkali Compounds $Li_3OMC_5H_5$ (M = Be, Mg, and Ca): How to Increase the Aromaticity of Li_3^+ Ring?

YIN-FENG WANG, WEI CHEN, GUANG-TAO YU, ZHI-RU LI, CHIA-CHUNG SUN

State Key Laboratory of Theoretical and Computational Chemistry, Institute of Theoretical Chemistry, Jilin University, Changchun 130023, People's Republic of China

Received 25 March 2009; accepted 4 May 2009
Published online 3 November 2009 in Wiley InterScience (www.interscience.wiley.com).
DOI 10.1002/qua.22349

ABSTRACT: The structures of novel metal-[metal oxide]-nonmetal sandwich-like superalkali compounds, that is, H- and T-shaped $Li_3OMC_5H_5$ (M = Be, Mg, and Ca), with all the real frequencies are obtained for the first time at the MP2/6-311+G(2d, p) level. For M = Be, the T-shaped isomer is more stable than the H-shaped one, but the H-shaped isomer is more stable than the T-shaped one for M = Mg and Ca. The natural bond orbital analysis indicates that these compounds are complex zwitterions and can be denoted as $(Li_3)^+(O^{2-}M^{2+})(C_5H_5)^-$ with two aromatic rings (Li_3^+ and $C_5H_5^-$). Four factors to increase the nucleus-independent chemical shift (NICS) of Li_3^+ ring in $Li_3OMC_5H_5$ systems are found. (1) Replacing the T-shaped structure with parallel Li_3^+ and $C_5H_5^-$ ring by the corresponding H-shaped structure with perpendicular Li_3^+ and $C_5H_5^-$ ring, the NICS value considerably increases from $-7.8 \sim -8.2$ to $-22.2 \sim -43.4$ ppm. (2) The existence of the neighboring alkaline earth metal oxide subunit evidently increases the NICS in H-shaped structures from about -11.1 to $-16.1 \sim -37.0$ ppm. (3) Based on the finding that the alkaline earth atomic number dependence of the aromaticity of Li_3^+ ring, the larger atomic number increases the NICS value. (4) The end $C_5H_5^-$ subunit increases the NICS value. For example, the increase is -6.4 ppm for H-shaped $Li_3OCaC_5H_5$. In addition, the expected out-of-plane σ-aromaticity of Li_3^+ ring is not exhibited, in contrast to that in the sandwich-like structure of Li_3OLi_3 (Chen et al., J Chem Phys, 2005, 123, 164306), but the in-plane σ-aromaticity of it is increased. Why? This is because (1) the size of the OM subunit near the Li_3^+ ring is small, and (2) the large-sized $C_5H_5^-$ subunit is far from the Li_3^+ ring. For these

Correspondence to: Z.-R. Li; e-mail: lzr@jlu.edu.cn
Contract grant sponsor: National Natural Science Foundation of China.
Contract grant numbers: 20773046, 20573043.
Additional Supporting Information may be found in the online version of this article.

$Li_3OMC_5H_5$, the H-shaped structure exhibits electride characteristics, and the T-shaped structure with lithium anion exhibits alkalide characteristics.
Int J Quantum Chem 110: 1953–1963, 2010

Key words: metal-[metal oxide]-nonmetal; sandwich-like compound; superalkali; aromaticity; NICS

1. Introduction

More than 2 decades ago, Boldyrev and Gutsev introduce the concepts of superhalogens [1(a,b)] and superalkali [1(b,c)]. Since Bergeron et al. [2, 3] found that a cluster of 13 aluminum atoms behaves like a single iodine atom, and that a cluster of 14 aluminum atoms behaves like an alkaline earth atom, superatoms have become basic units in chemistry and have recently attracted more and more attention. As a novel kind of chemical species, the superatoms open unexpected research areas. All-metal aromatic superatoms, recently synthesized by Li et al. [4], constitute one such example. The concept of unusual multiple-fold aromaticity including σ- and π-aromaticity is reported [5, 6]. The unusual aromaticity of all-metal superatoms [4–7], such as Li_3^+, Al_4^{2-}, and Al_3^- as well as nonmetal superatoms (N_3^- and N_4^{2-}) [8, 9], has been studied.

Recently, the sandwich-like compounds [9–18] with superatoms have been an upsurge of interest because of their distinctive topologic structures and unusual properties, for example, the unusual aromaticity [11, 12(c)–15(b), 16]. Notice that, the metal-nonmetal-metal sandwich-like Li_3OLi_3 [14(b)] exhibits charming out-of-plane σ-aromaticity, in which the maximum nucleus-independent chemical shift ($NICS_{max}$) value of σ-aromatic ring Li_3^+ shifts from the center of the ring to the outside of the ring plane about 2.5 Å.

Some superatom compounds [14(b), 15(a,c)] with superalkali end ring may have electride [19] or alkalide [19(c), 20] characteristics. Electrides are a novel kind of ionic salts in which anionic sites are occupied solely by electrons [19]. Alkalides are compounds containing anionic alkali metals (e.g., Na^-, K^-, Rb^-, or Cs^-) [20]. The metal-nonmetal-metal sandwich-like Li_3OLi_3 [14(b)] and metal-nonmetal-metal Li_3N_3Be [15(a)] are new type sandwich-like electride superatom compounds or supermolecules [15(a)]. In addition, some structures of the superalkali superhalogen compounds $(Li_3)^+(SH)^-$ (SH = LiF_2, BeF_3, and BF_4) [15(c)] are electride superatom compounds, whereas the others are alkalide superatom.

These sandwich-like compounds with super atoms may be classified into four modes type: all-metal type [11–13(a)], nonmetal-metal-metal type [13(a,b)], metal-nonmetal-metal type [9(a), 14, 15(b)], and nonmetal-metal-nonmetal type [16–18].

However, whether or not a novel sandwich-like modes type, metal-[metal oxide]-nonmetal exists? In this article, we have used the alkaline earth metal oxide, that is, BeO, MgO, and CaO, to be sandwiched between the metallic Li_3^+ (toward the oxygen atom) and the nonmetallic $C_5H_5^-$ ring (toward the alkaline-earth metal atom) to form two kinds of structures. These metal-[metal oxide]-nonmetal sandwich-like superatom compounds may have interesting aromaticities because of the interactions among the subunits and may be used as building blocks of material because of their zwitterionic characteristics.

This article aims at exploring the structure and the stability of these metal-[metal oxide]-nonmetal sandwich-like $Li_3OMC_5H_5$, revealing the influencing factors for the aromaticity of Li_3^+ ring, showing the existence conditions for the expected out-of-plane σ-aromaticity of Li_3^+, and exhibiting the electride or alkalide characteristics of these metal-[metal oxide]-nonmetal sandwich-like superalkali compounds.

2. Computational Methods

The geometries of the six $Li_3OMC_5H_5$ (M = Be, Mg, and Ca) were optimized, and the vibrational frequencies were calculated by the second-order Møller–Plesset perturbation theory (MP2) [21] level with 6-311+G (2d, p) basis set [22]. The natural bond orbital (NBO) [23] analysis by the MP2/6-311+G (2d, p) method was performed to provide an insight into the bonding nature of these compounds. The NICS [24, 25] was obtained by the GIAO-B3LYP/6-311+G (2d, p) method. The vertical ionization energies (VIEs) were determined at MP2/6-311+G (2d, p) by using Eq. (1), where $E[(Li_3OMC_5H_5)^+]$ is the energy of the $(Li_3OMC_5H_5)^+$ cation calculated with the same geometry of its counterpart of $Li_3OMC_5H_5$.

$$\mathrm{VIE} = E[(Li_3OMC_5H_5)^+] - E[Li_3OMC_5H_5] \quad (1)$$

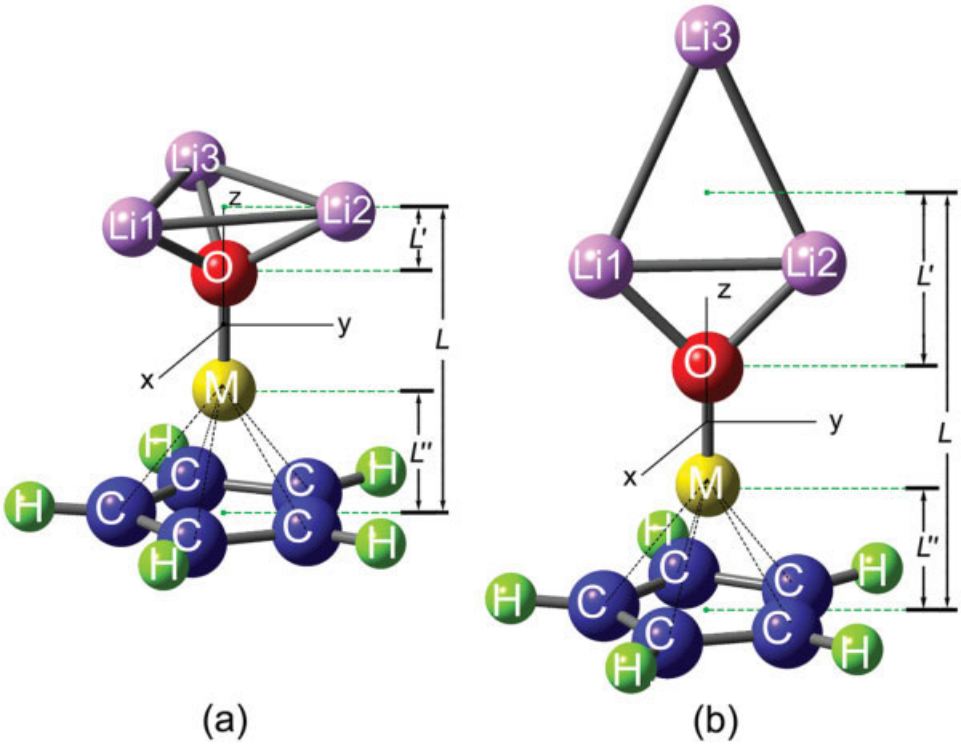

FIGURE 1. (a) H-shaped and (b) T-shaped structure for the $Li_3OMC_5H_5$ (M = Be, Mg, and Ca). [Color figure can be viewed in the online issue, which is available at www.interscience.wiley.com.]

The calculations were carried out with Gaussian 03 [26(a)] program package. The molecular structures and molecular orbitals were plotted with GaussView program [26(b)].

3. Results and Discussion

3.1. STRUCTURES CHARACTERISTICS AND VIBRATIONAL FEATURES

3.1.1. Equilibrium Geometries and Relative Stabilities

The optimized structures for the two kinds of $Li_3OMC_5H_5$ (M = Be, Mg, and Ca), which are confirmed by all real frequencies, are shown in Figure 1, and their geometric parameters are listed in Table I.

As shown in Figure 1, in the two kinds of $Li_3OMC_5H_5$ (M = Be, Mg, and Ca), the alkaline-earth metal oxide OM is sandwiched between the metallic Li_3 ring (toward the oxygen atom) and the nonmetallic C_5H_5 ring (toward the alkaline-earth metal atom). From Figure 1, the Li_3 and C_5H_5 ring in the first structure are parallel and both vertical to metal oxide OM. It just likes the letter "H" if it is transverse and this structure may be called H-shaped $Li_3OMC_5H_5$. The second structure may be called T-shaped $Li_3OMC_5H_5$ as the Li_3 and OM are in a plane and vertical to the C_5H_5 ring. It just likes the letter "T" if it is reversal.

For the H-shaped $Li_3OMC_5H_5$ (M = Be, Mg, and Ca), the Li_3 ring is regular triangular and the shape of Li_3O is regular pyramid. Four structural change

TABLE I
Optimized geometrical parameters of Li3OMC5H5 (in Å) at MP2/6-311+G (2d, p) level.

	H-shaped			T-shaped		
	Be	Mg	Ca	Be	Mg	Ca
Li1—Li2	2.720	2.846	2.880	2.456	2.445	2.412
Li1—Li3	2.720	2.846	2.880	3.094	3.093	3.093
Li1—O	1.835	1.799	1.783	1.767	1.764	1.769
L′	0.949	0.733	0.634	2.217	2.219	2.244
O—M	1.492	1.901	2.221	1.453	1.834	2.089
L″	1.530	2.037	2.370	1.555	2.015	2.368
L	3.971	4.671	5.225	5.225	6.068	6.701
C—C	1.422	1.423	1.420	1.421	1.423	1.420
C—H	1.081	1.083	1.084	1.081	1.083	1.084

characteristics, from M = Be to Ca, are shown in Table I. (1) The Li—Li bond length slightly increases from 2.720 to 2.880 Å. (2) The layer distance between Li_3 ring and O atom (L') decreases from 0.949 to 0.634 Å. (3) The O—M bond length increases from 1.492 to 2.221 Å because of increase of the ionic radii of M. (4) The layer distance between M atom and C_5H_5 ring (L'') increases from 1.530 to 2.370 Å also because of increase of the ionic radii of M. As a result, the distance between the Li_3 and C_5H_5 ring (L) increases from 3.971 to 5.225 Å.

In the T-shaped $Li_3OMC_5H_5$ (M = Be, Mg, and Ca), the Li_3 ring is isosceles triangular and two Li atoms are near to but the other is away from the O atom. Four structural change characteristics, from M = Be to Ca, are also shown in Table I. (1) The Li1—Li2 bond length slightly decreases from 2.456 to 2.412 Å. (2) The layer distance between Li_3 ring and O atom (L') slightly increases from 2.217 to 2.244 Å. (3) The O—M bond length increases from 1.453 to 2.089 Å. (4) the layer distance between M atom and C_5H_5 ring (L'') increases from 1.555 to 2.368 Å. As a result, the distance between the Li_3 and C_5H_5 ring (L) increases from 5.225 to 6.701 Å.

Obviously, the geometries of the C_5H_5 rings in $Li_3OMC_5H_5$ are almost the same because of the far distance between the Li_3 and C_5H_5 ring ($L > 3.9$ Å), although the change is large from two parallel rings (Li_3^+ and $C_5H_5^-$) in H-shaped to the perpendicular rings in T-shaped structure. Likewise, the effect of OM on C_5H_5 geometry is also very small because of the far distance between the OM and C_5H_5 ring and the small size of OM in each structure ($L'' > 1.5$ Å).

To understand the relative stability, we consider the changes of the total energies for the H- and T-shaped $Li_3OMC_5H_5$ from M = Be to Ca. From Figure 2, the energy of T-shaped isomer is lower than that of H-shaped one for M = Be, which indicates that the T-shaped $Li_3OBeC_5H_5$ is more stable than the H-shaped one. However, for M = Mg and Ca, the energy of H-shaped isomer is lower than that of the corresponding T-shaped one, which indicates that the H-shaped isomer is more stable than the corresponding T-shaped one for M = Mg and Ca. Obviously, the H-shaped structures with large atomic number of M are stable.

3.1.2. Vibrational Features

The results of the infrared spectra may be used for experimental identification of these metal-[metal oxide]-nonmetal sandwich-like superalkali superatom compounds. The infrared spectra of the H- and T-shaped $Li_3OMC_5H_5$ are shown in Supporting Information Figures S1(a) and S2(a), respectively. Four characteristic peaks of each $Li_3OMC_5H_5$ are selected, in which each peak obviously changes with the change of M from Be to Ca. The four corresponding characteristic vibrational modes for H- and T-shaped $Li_3OMC_5H_5$ are illustrated in Supporting Information Figures S1(b) and S2(b), respectively.

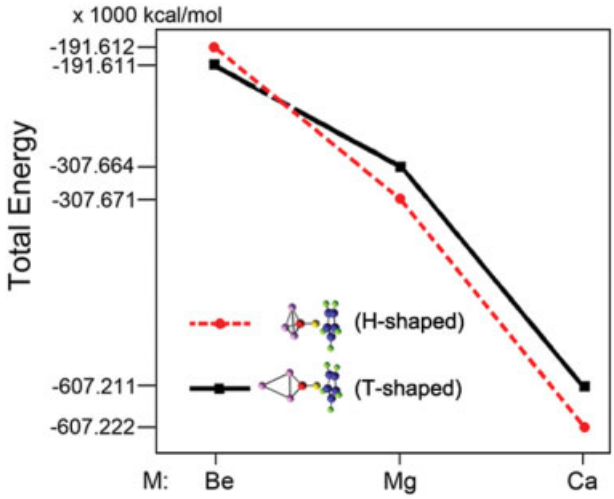

FIGURE 2. The changes of the total energies for the H- and T-shaped $Li_3OMC_5H_5$ along with the change of M from Be to Ca. [Color figure can be viewed in the online issue, which is available at www.interscience.wiley.com.]

3.2. NBO ANALYSIS

The NBO charges for the $Li_3OMC_5H_5$ (M = Be, Mg, and Ca) at MP2/6-311+G (2d, p) level are listed in Table II.

From Table II, for H-shaped $Li_3OMC_5H_5$, the charges of the three Li atoms in each Li_3 ring are identical and positive (0.335 ~ 0.407). The range of charges of the Li_3 rings is around 1.006 ~ 1.224. For the T-shaped $Li_3OMC_5H_5$, the charge of Li3 atom is negative (−0.360 ~ −0.356), and the values of charges of Li1 and Li2 are large positive ones (0.657 ~ 0.667). As a result, the charges of Li_3^+ rings are still positive (0.958 ~ 0.970). These results show the valence of Li_3 superatom is +1. For these $Li_3OMC_5H_5$, the ranges of the charges of O and M are, respectively, around −1.834 ~ −1.970 and 1.652 ~ 1.879, which indicate the valences of the O and M are −2 and +2, respectively. Likewise, the range of charge of the C_5H_5 rings of −0.860 ~

TABLE II

Natural bond orbital (NBO) charges at MP2/6-311+G (2d, p) level.

	H-shaped			T-shaped		
	Be	Mg	Ca	Be	Mg	Ca
Li1	0.335	0.374	0.407	0.667	0.661	0.657
Li3	0.335	0.374	0.407	−0.360	−0.358	−0.356
Li_3 ring	1.006	1.123	1.224	0.974	0.965	0.958
O	−1.908	−1.970	−1.962	−1.834	−1.908	−1.907
M	1.762	1.756 (1.599)	1.652 (1.013)	1.732	1.859 (1.713)	1.879(1.646)
C_5H_5 ring	−0.860	−0.910	−0.914	−0.867	−0.915	−0.931

The values in parentheses are the values for the $Li_3OMC_5H_5$ mode, in which the Mg and Ca in $Li_3OMC_5H_5$ replaced by Be directly, see text.

−0.931 indicates that the valence of C_5H_5 ring in each structure is −1. Thus, these $Li_3OMC_5H_5$ can be denoted as $(Li_3)^+(O^{2-}M^{2+})(C_5H_5)^-$. In this case, the Li_3 ring loses an electron and C_5H_5 gains an electron to form two aromatic Li_3^+ ring and $C_5H_5^-$ ring. The OM may play a role of the charge-transfer bridge. These metal-[metal oxide]-nonmetal sandwich-like superalkali compounds are charge-separated systems, and thus, they are complex zwitterions. As a result, they may be used as building blocks of material.

Considering the effect of ionization potential (IP), the smaller the IP of M atom, the larger the charge of M in $Li_3OMC_5H_5$ should be. However, it can be seen in Table II, from M = Be to Ca, the charge of M obviously decreases for H-shaped $Li_3OMC_5H_5$ (from 1.762 to 1.652) but obviously increases for T-shaped $Li_3OMC_5H_5$ (from 1.732 to 1.879). Why? It is found that two contrary influencing factors effect on the charges of M in different $Li_3OMC_5H_5$. (1) The decrease of IP, 9.320 (Be) > 7.644 (Mg) > 6.111 eV (Ca) [27], may lead to the increase of the charge of M. (2) The increase of the bond lengths of O—M may lead to the decrease of charge of M.

To further understand the effect of bond length on the charge of M, we design two series of $Li_3OMC_5H_5$ modes to calculate the charge of M. Fixing the equilibrium geometries of H- and T-shaped $Li_3OMC_5H_5$ (M = Be, Mg, and Ca) and substituting the M atoms by Be atom, the two series of $Li_3OMC_5H_5$ modes are constructed. Thus, in H-shaped $Li_3OMC_5H_5$ mode series, the distances of O—Be are 1.492 from O—Be, 1.901 from O—Mg, and 2.221 Å from O—Ca. Likewise, in T-shaped $Li_3OMC_5H_5$ mode series, the distances of O—Be are 1.453 from O—Be, 1.834 from O—Mg, and 2.089 Å from O—Ca.

The NBO charges of the Be atoms in two series of $Li_3OMC_5H_5$ modes are calculated at MP2/6-311+G (2d, p) level and are also listed in Table II to show the change of the charge of M along with the increase of bond lengths of O—M. The results show that the charge of M decreases along with the increase of bond lengths of O—M in two series of $Li_3OMC_5H_5$ modes (see Supporting Information Fig. S3).

From Supporting Information Figure S3(a), the decrease of the charge of M coming from the effect of the bond lengths of O—M in the mode systems accords with the decrease of the charge of M in the H-shaped $Li_3OMC_5H_5$, which shows that the change of charge of M for H-shaped $Li_3OMC_5H_5$ mainly comes from the effect of the bond lengths of O—M (from M = Be to M = Ca).

From Supporting Information Figure S3(b), the decrease of the charge of M coming from the effect of the bond lengths of O—M in the mode systems does not accord with the increase of the charge of M in the T-shaped $Li_3OMC_5H_5$, which shows that the change of charge of M for T-shaped $Li_3OMC_5H_5$ mainly does not come from the effect of the bond lengths of O—M (from M = Be to M = Ca) but the effect of IP on M atom charge (from M = Be to M = Ca).

3.3. AROMATICITY FOR THE $Li_3OMC_5H_5$

The NICS, proposed by Schleyer and Boldyrev [24, 25], is an efficient and simple criterion for probing aromaticity, which is based on the negative value of the magnetic shielding computed, for example, at or above the geometrical centers of rings or clusters. Systems with (significant) negative NICS values are aromatic, and systems with

TABLE III

Nucleus-independent chemical shifts (NICS(0)) (in ppm) with the GIAO-B3LYP/6-311+G (2d, p) level.

	H-shaped			T-shaped		
	Be	Mg	Ca	Be	Mg	Ca
Li_3^+[a]	−11.0	−11.1	−11.1	−10.8	−10.8	−10.8
Li_3^+ in Li_3^+OM[a]	−16.1	−29.5	−37.0	−6.6	−6.7	−7.8
Li_3^+ in $Li_3OMC_5H_5$	−22.2	−34.4	−43.4	−7.7	−7.8	−8.2
$C_5H_5^-$ in $Li_3OMC_5H_5$	−17.2	−15.0	−16.0	−14.9	−11.8	−14.1

[a] The NICS values are obtained for Li_3^+ and Li_3^+OM by simply removing the OMC_5H_5 and $C_5H_5^-$ from the corresponding $Li_3OMC_5H_5$ structure, respectively.

strongly positive NICS values are antiaromatic. The more negative the NICS value, the more aromatic the system. In this study, the NICS values are evaluated with the GIAO-B3LYP/6-311+G (2d, p) method by placing ghost atoms at the geometric centers of the Li_3 and C_5H_5 in the six structures.

3.3.1. Aromaticity of Li_3^+ Ring in $LI_3OMC_5H_5$

As shown in Table III, the ranges of the NICS are $-22.2 \sim -43.4$ and $-7.7 \sim -8.2$ ppm for H- and T-shaped $Li_3OMC_5H_5$, respectively. All the negative NICS values for them suggest the existences of electron delocalizations and strong aromaticities.

For the regular triangular Li_3^+ ring, the σ-aromaticity in the bare Li_3^+ cation has been reported by Alexandrova and Boldyrev [7(b)]. In the H-shaped $Li_3OMC_5H_5$ (M = Be, Mg, and Ca), the HOMO [see Fig. 3(a)] of the regular triangular Li_3^+ subunit is a delocalized σ-bonding orbital that is formed from the 2s atomic orbitals of three Li atoms. Owing to the valence of +1 for the Li_3^+ subunit, this delocalized σ-bonding orbital is occupied by two electrons, which satisfies the $4n + 2$ electron counting rule and indicates the σ-aromatic nature [7(b)] of the Li_3^+ subunit in each H-shaped $Li_3OMC_5H_5$ (M = Be, Mg, and Ca).

In the T-shaped $Li_3OBeC_5H_5$ (M = Be, Mg, and Ca), the regular triangular Li_3^+ ring is changed into the isosceles triangular Li_3^+ ring. Its HOMO is still a delocalized σ-bonding orbital [see Fig. 3(b)]. This delocalized σ-bonding orbital is also occupied by two electrons, which satisfies the $4n + 2$ electron counting rule. Therefore, the Li_3^+ subunits are σ-aromatic for the T-shaped $Li_3OMC_5H_5$ (M = Be, Mg, and Ca).

3.3.2. Influencing Factors for the Aromaticity of Li_3^+ Ring

To further understand the effect of subunits on the aromaticities of Li_3^+ rings in the H- and T-shaped $Li_3OMC_5H_5$ (M = Be, Mg, and Ca), we have used the bare Li_3^+ and $Li_3^+\cdots OM$ subunit, the structures of which are obtained by simply removing the OMC_5H_5 and $C_5H_5^-$ from the H- and T-shaped $Li_3OMC_5H_5$ structures, respectively. The NICS values at the centers of Li_3^+ ring in the bare Li_3^+ and Li_3^+OM subunit are calculated at B3LYP/6-311+G (2d, p), and the results are also listed in Table III. The different effects of subunits on the NICS of Li_3^+ ring are illustrated in Supporting Information Figures S4(a) and (b).

As shown in Table III, the NICS values of $-22.2 \sim -43.4$ of Li_3^+ rings in H-shaped $Li_3OMC_5H_5$ are obviously larger than that of $-7.7 \sim -8.2$ ppm of Li_3^+ rings in T-shaped $Li_3OMC_5H_5$ (M = Be, Mg, and Ca).

For the H-shaped structures, as the Li_3 ring is perpendicular to OM subunit, under the repulsing effect of OM subunit, the degree of the delocalization of the σ-bonding orbital of the Li_3 ring (HOMO) is almost not changed. Furthermore, the Li_3 ring subunit shares the electron cloud of OM subunit in HOMO-3 [see Fig. 3(c)]. In HOMO-3, a lobe of the p orbital (from the 2p orbital of O atom in OM subunit) envelops Li_3^+ ring subunit. Similarly, the π-orbital of C_5H_5 subunit [HOMO-6 in Fig. 3(e)] also provides a little sharing of the electron cloud for Li_3 ring subunit. Because the OM and C_5H_5 subunits provide the additional contributions of σ-bonding delocalized electron clouds for Li_3 ring subunit, the NICS of Li_3^+ ring subunit is considerably increased comparing to that of bare Li_3^+ ring (−11.1 ppm).

For the T-shaped structures, as the Li_3 ring is coplanar to OM subunit, under the repulsing effect of OM subunit, the center of the electron cloud is shifted toward the Li3 atom, and the degree of the delocalization of the σ-bonding orbital of the Li_3 ring [HOMO in Fig. 3(b)] is obviously decreased.

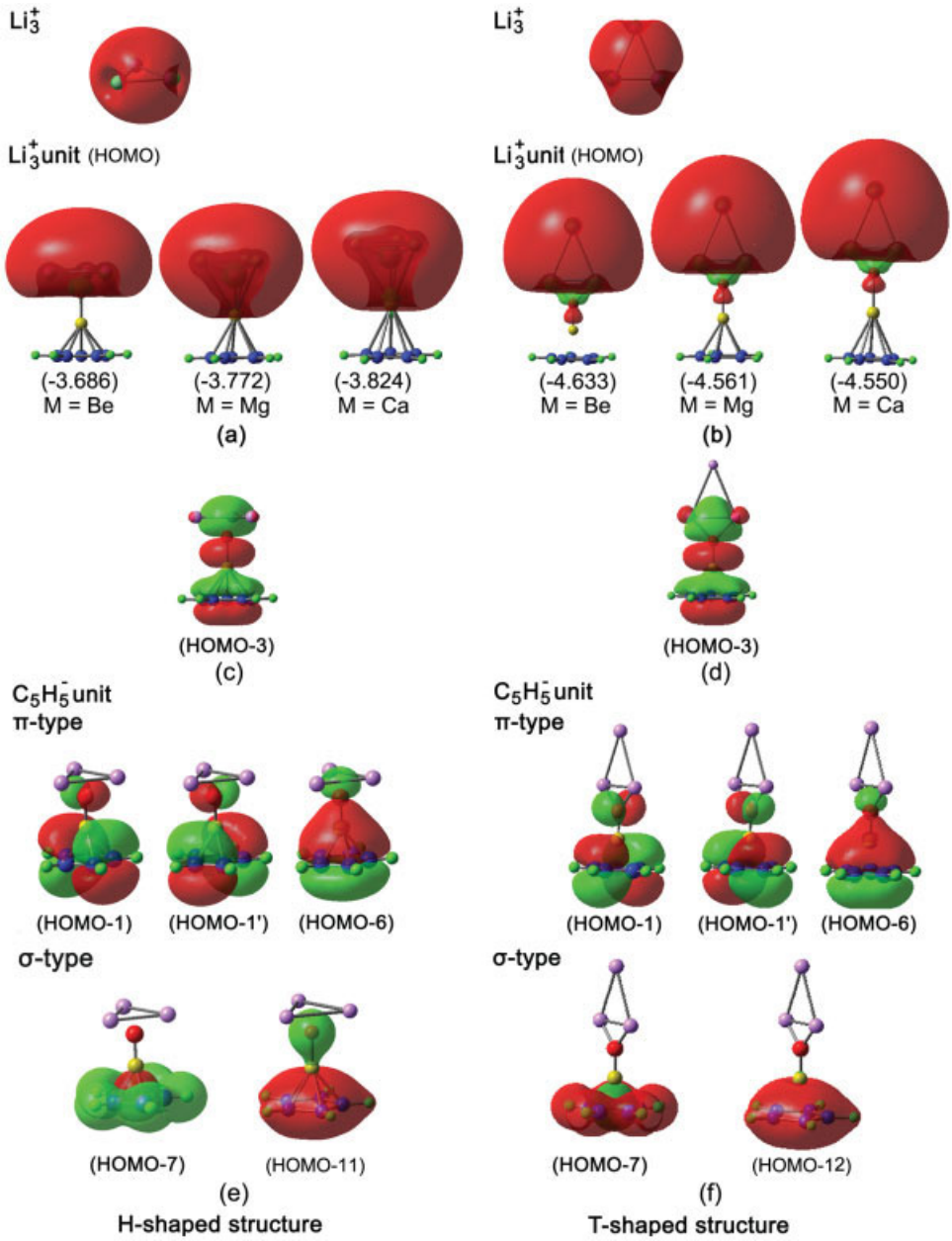

FIGURE 3. Selected molecular orbitals. Orbital energies (in eV) in parentheses. [Color figure can be viewed in the online issue, which is available at www.interscience.wiley.com.]

Although the Li_3 ring may slightly share the σ-bonding electron clouds from HOMO-3 [Fig. 3(d)] and HOMO-6 [Fig. 3(f)], the NICS of Li_3^+ ring subunit is still obviously decreased comparing to that of bare Li_3^+ ring (−10.8 ppm).

Therefore, the shape of structure (H- or T-shaped) is an important influencing factor to effect on the aromaticity of Li_3^+ ring because of the interaction between the subunits with different relative orientations.

In the H-shaped $Li_3OMC_5H_5$, from Table III, the range of −16.4 ~ −37.0 ppm for the NICS of the Li_3^+ rings of the Li_3^+OM (M = Be, Mg, and Ca) subunit is much larger than that of bare regular triangular Li_3^+ ring subunit (about −11.1 ppm). In the T-shaped $Li_3OMC_5H_5$, from Table III, the range of

$-6.6 \sim -7.8$ ppm for the NICS of the Li_3^+ rings of the Li_3^+OM (M = Be, Mg, and Ca) subunit is smaller than that of bare isosceles triangular Li_3^+ ring (-10.8 ppm) subunit. These data indicate that alkaline earth metal oxide (OM) subunit considerably increases the aromaticity of the Li_3^+ ring in H-shaped structures [see Supporting Information Fig. S4(a)] but decreases that in T-shaped structures [see Supporting Information Fig. S4(b)].

Therefore, the alkaline earth metal oxide is also an important influencing factor to effect on the aromaticity of Li_3^+ ring.

In H-shaped $Li_3OMC_5H_5$, the NICS value at the center of Li_3^+ ring considerably increases from M = Be to M = Ca (-22.2 for M = Be < -34.4 for M = Mg < -43.4 for M = Ca), and that slightly increases from M = Be to M = Ca (-7.7 for M = Be < -7.8 for M = Mg < -8.2 for M = Ca) in T-shaped ones, which show an alkaline earth metal atomic number dependence of the NICS value for the Li_3^+ ring. This may be understood from the HOMOs in Figures 3(a) and (b). For H-shaped structures, from M = Be to Ca, the degree of the delocalization of the HOMO [see Fig. 3(a)] obviously increases. Likewise, for T-shaped structures, from M = Be to Ca, the degree of the delocalization of the HOMO [see Fig. 3(b)] slightly increases.

The alkaline earth atomic number dependence of the aromaticity of Li_3^+ ring shows that the alkaline earth atomic number is another important influencing factor to effect on the aromaticity of Li_3^+ ring.

Supporting Information Figure S4(a) illustrates that the NICS of the Li_3^+ rings of the Li_3^+OM subunit and that of about $-5 \sim -6$ ppm for the contribution of $C_5H_5^-$ ring subunit is the NICS of the H-shaped $Li_3OMC_5H_5$. Similarly, Supporting Information Figure S4(b) illustrates that the NICS of the Li_3^+ rings of the Li_3^+OM subunit and that of about -1 ppm for the contribution of $C_5H_5^-$ subunit is the NICS of the T-shaped $Li_3OMC_5H_5$. These indicate that the end $C_5H_5^-$ subunit can increase the NICS of Li_3^+ ring and is also an important influencing factor to effect on the aromaticity of Li_3^+ ring.

As discussed earlier, four important influencing factors for the aromaticity of Li_3^+ ring are found.

3.3.3. LOCATION AND MAGNITUDE OF $NICS_{max}$ FOR Li_3^+ RING

In our previous works, the metal-nonmetal-metal sandwich-like Li_3OLi_3 [13(b)] exhibits the charming out-of-plane σ-aromaticity, in which the $NICS_{max}$ value of σ-aromatic rings Li_3^+ shifts from the center of the ring to the outside of the ring plane about 2.5 Å. Obviously, in these H-shaped metal-[metal oxide]-nonmetal sandwich-like $Li_3OMC_5H_5$ structure (M = Be, Mg, and Ca), the Li_3 ring also has a neighboring O atom, which is similar to that in the Li_3OLi_3 structure. For the electron clouds in HOMOs, they are also similar between H-shaped $Li_3OMC_5H_5$ and Li_3OLi_3. So, may the out-of-plane σ-aromaticity of the Li_3^+ rings in the H-shaped $Li_3OMC_5H_5$ also be exhibited? Unfortunately, the expected out-of-plane σ-aromaticity of Li_3^+ ring is not exhibited. From Supporting Information Figure S5(a), just like the bare Li_3^+ ring, the $NICS_{max}$ appears at the center of the Li_3^+ ring in the three H-shaped $Li_3OMC_5H_5$ ($L_0 = 0$), showing the in-plane σ-aromaticity. Why?

We take three models from equilibrium geometry of the H-shaped $Li_3OBeC_5H_5$ and the model part is kept the same as that in the equilibrium geometry, that is, Li_3^+O with the short $Li_3^+\cdots O$ distance (0.949 Å), Li_3^+OBe with the short $Li_3^+\cdots Be$ distance (2.441 Å), and $Li_3^+C_5H_5^-$ with the long $Li_3^+\cdots C_5H_5^-$ distance (3.971 Å). From Supporting Information Figure S5(b), all the $NICS_{max}$ values are located at the center of the Li_3^+ ring ($L_0 = 0$) in $Li_3OBeC_5H_5$ and the relative subunit models. Although the small O and OBe subunit are near the Li_3 subunit, they do not lead to out-of-plane σ-aromaticity of Li_3^+ ring may be due to the small sizes of them. The large $C_5H_5^-$ and $OBeC_5H_5^-$ subunit are far away from Li_3 subunit and they also do not lead to out-of-plane σ-aromaticity of Li_3^+ ring.

Can the large subunit with a small distance between the Li_3^+ ring and the subunit make the Li_3^+ ring exhibit out-of-plane σ-aromaticity? From Supporting Information Figure S5(c), when the distance between Li_3^+ and $C_5H_5^-$ ring subunit L_1 is long 3.971 Å (from $Li_3OBeC_5H_5$ structure), the out-of-plane σ-aromaticity is not exhibited. When the L_1 is as short as 1.5 Å, the out-of-plane σ-aromaticity with $L_0 = 1.0$ Å ($NICS_{max}$ apart from the center of Li_3^+ ring by 1.0 Å) is obviously exhibited. Thus, large $C_5H_5^-$ ring subunit can lead to out-of-plane σ-aromaticity of Li_3^+ ring when it is close to the Li_3^+ ring.

In these metal-[metal oxide]-nonmetal sandwich-like structures of $Li_3OMC_5H_5$ (M = Be, Mg, and Ca), the expected out-of-plane σ-aromaticity of Li_3^+ ring is not exhibited, but the increase of the in-plane σ-aromaticity of it is exhibited. This is because (1) the size of the OM subunit near the Li_3^+ ring is small, and (2) the large-sized $C_5H_5^-$ subunit is far from the Li_3^+ ring.

3.3.4. Triple-Fold Aromaticity (π, σ_p, and σ_s) of $C_5H_5^-$ Ring

For the $C_5H_5^-$ ring, the aromaticity and the MOs have been reported [28, 29]. In $Li_3OMC_5H_5$ (M = Be, Mg, and Ca), as shown in Table III, the range of the NICS values at the centers of $C_5H_5^-$ ring subunits for H-shaped structures with parallel Li_3^+ and $C_5H_5^-$ ring ($-15.0 \sim -17.2$ ppm) is larger than that for T-shaped ones with perpendicular Li_3^+ and $C_5H_5^-$ ring ($-11.8 \sim -14.9$ ppm). This indicates that the shape of structure is an important influencing factor to effect on the aromaticity of $C_5H_5^-$ ring because of the interaction between the end subunits in the structure.

From Supporting Information Figure S5(a), it is shown that the bare Li_3^+ ring and the Li_3^+ ring in H-shaped $Li_3OMC_5H_5$ (M = Be, Mg, and Ca) are usually σ-aromatic as the $NICS_{max}$ is located at the center of the ring ($L_0 = 0$). Although the $NICS_{max}$ of classical π-aromatic benzene ring is located at 1.0 Å above the center of the ring plane [28(a)], which shows that the classical π-aromaticity is out-of-plane. From Supporting Information Figure S6(a), the NICS value of $C_5H_5^-$ subunit of H-shaped $Li_3OBeC_5H_5$ (the black line) illustrates that the $NICS_{max}$ is located at the center of the $C_5H_5^-$ ring ($L_0 = 0$), which is similar to that of the usual σ-aromatic Li_3^+ ring. This indicates that the π-aromatic $C_5H_5^-$ ring subunit not only has the π-aromaticity but also owns the σ-aromaticity.

It is reported [28(a)] that the principal component of the NICS tensor zz represents the π-aromaticity, whereas xx and yy represent the σ-aromaticity.

$$\text{We can write the } NICS_{\pi+\sigma} = NICS_{\pi} + NICS_{\sigma} = (zz)/3 + (xx + yy)/3$$

For $C_5H_5^-$ subunit in H-shaped $Li_3OBeC_5H_5$, from Supporting Information Figure S6(a), at 1.0 Å above the center of the ring plane ($L_0 = 1.0$), the $NICS_{\pi}$ ($(zz)/3$ of -11.3 ppm) is the largest, but the $NICS_{\sigma}$ is a positive value ($(xx + yy)/3$ of 0.7 ppm). As a result, the value of the $NICS_{\pi+\sigma}$ is -10.6 ppm, not the largest. At the center of the $C_5H_5^-$ ring ($L_0 = 0$), the $NICS_{\sigma}$ of -10.3 ppm is the largest, and the $NICS_{\pi}$ is a negative value of -6.9 ppm, which results in the largest $NICS_{\pi+\sigma}$ of -17.2 ppm, that is, $NICS_{max}$ (see Table III). According to the three values, we may provide a rough estimation that σ-aromaticity and π-aromaticity are 66 and 34%, respectively.

To further understand the aromatic nature of $C_5H_5^-$ subunit, the MOs mainly from the $C_5H_5^-$ subunit are analyzed. Removing the bonding/antibonding orbital pair(s), the five selected MOs for $Li_3OBeC_5H_5$ are depicted in Figure 3(e) or (f). From Figure 3(e) (or f), the five MOs can be divided into three types. The first type includes three π-bonding orbitals, HOMO-1, HOMO-1′, and HOMO-6, which are formed from the out-of-plane 2p orbitals. Those three π-MOs are occupied by six π-electrons, which give π-aromaticity to the $C_5H_5^-$ ring of each molecule according to the $4n + 2$ electron counting rule. The second type is formed from the in-plane 2p orbital and is a σ_p bonding orbital (HOMO-7). The third type is mainly formed from the 2s orbital and is a σ_s bonding orbital (HOMO-11 for H- and HOMO-12 for T-shaped structure). Each of the two types has two electrons, satisfying the $4n + 2$ electron counting rule. Therefore, the $C_5H_5^-$ ring subunit has three independent delocalized bonding systems, one π and two σ. This indicates that the $C_5H_5^-$ ring subunit is triple-fold aromaticity (π, σ_p, and σ_s).

Recently, to exhibit the chemical intuition, a newly developed adaptive natural density partitioning (AdNDP) method [29(a)] has been applied to a series of organic aromatic molecules including $C_5H_5^-$[29(b)]. The AdNDP representation of aromatic systems seamlessly incorporates localized and delocalized bonding elements. For the $C_5H_5^-$, the bonding pattern revealed by AdNDP [29(b)] closely resembles parental canonical MOs (π, σ_p, and σ_s in Fig. 3), which gives a support for the triple-fold aromaticity of the $C_5H_5^-$ ring.

These MOs of $Li_3OBeC_5H_5$ are similar to the corresponding MOs of the $Li_3OMgC_5H_5$ and $Li_3OCaC_5H_5$. Similarly, the triple-fold aromaticity (π, σ_p, and σ_s) is also exhibited in $Li_3OMgC_5H_5$ and $Li_3OCaC_5H_5$.

3.4. VERTICAL IONIZATION ENERGIES

The VIEs of the H- and T-shaped $Li_3OMC_5H_5$ (M = Be, Mg, and Ca) obtained at MP2/6-311+G (2d, p) level are presented in Table IV.

From Be to Ca, as tabulated in Table IV, the VIE values gradually increase for the H-shaped $Li_3OMC_5H_5$ (4.10 for M = Be <4.42 for Mg <4.5 eV for Ca) but gradually decrease for the T-shaped $Li_3OMC_5H_5$ (4.70 for M = Be <4.65 for Mg <4.61 eV for Ca). Figure 3(a) exhibits the energies of the HOMOs for these structures. Obviously, the order of the VIEs is in accordance with that of the HOMO energies for H- and T-shaped structures.

In addition, the (MP2-HF)/MP2 components represents the electron correlation contribution. From Ta-

TABLE IV

Vertical ionization energy (VIE) (in eV) for the six molecules at the MP2/6-311+G (2d, p) level.

	H-shaped			T-shaped		
	Be	Mg	Ca	Be	Mg	Ca
HF	3.26	3.51	3.61	4.04	3.97	3.96
MP2	4.10	4.42	4.50	4.70	4.65	4.61
(MP2-HF)/MP2	20.6%	20.6%	19.7%	14.0%	14.5%	14.2%

VIE = $E[(Li_3OMC_5H_5)^+] - E[Li_3OMC_5H_5]$.

ble IV, the electron correlation contribution for VIE is important. They are about 19.7 ~ 20.6% and 14.0 ~ 14.5% for H-and T-shaped $Li_3OMC_5H_5$, respectively.

For each H-shaped $Li_3OMC_5H_5$ (M = Be, Mg, and Ca),the HOMO mainly comes from the contribution of superatom subunit (Li_3) and is an excess electron orbital [see Fig. 3(a)] under the effect of $(O^{2-}M^{2+})(C_5H_5)^-$. As mentioned earlier, the VIE values of them (4.10 ~ 4.50 eV) are lower than that of the electride of Li_3N_3Be (4.73 eV) [15(a)] and that of $(Li3)^+(SH)^-$ (SH = LiF_2, BeF_3, and BF_4) (4.6 ~ 5.2 eV). [15(c)] Therefore, the H-shaped $Li_3OMC_5H_5$ exhibits electride characteristics.

For each T-shaped $Li_3OMC_5H_5$ (M = Be, Mg, and Ca),the HOMO mainly comes from the contribution of the superatom subunit (Li_3) under the effect of $(O^{2-}M^{2+})(C_5H_5)^-$ and is also an excess electron orbital [see Fig. 3(b)]. The electron clouds of Li_3 in the HOMO are pushed up by the $(O^{2-}M^{2+})(C_5H_5)^-$, which makes the Li3 atom (far from the $(O^{2-}M^{2+})(C_5H_5)^-$) become an alkali metal anion (see NBO charges in Table II). Furthermore, the VIE values of them (4.61 ~ 4.70 eV) are also lower than the alkalide of $(Li3)^+(SH)^-$ (SH = LiF_2, BeF_3, and BF_4) (5.4 ~ 6.1 eV) [15(c)]. Thus, the T-shaped $Li_3OMC_5H_5$ exhibits alkalide characteristics.

4. Conclusions

In this article, we design two kinds of structures for the metal-[metal oxide]-nonmetal sandwich-like superalkali compounds: H- and T-shaped $Li_3OMC_5H_5$ (M = Be, Mg, and Ca) at the MP2/6-311+G (2d, p) level for the first time. The key points of this work are summarized as follows:

1. Each structure of these compounds includes two aromatic ring subunits (the metallic Li_3^+ and nonmetallic $C_5H_5^-$) because of the separated charges. The metal oxide is sandwiched between the Li_3^+ ring (toward the oxygen atom) and the $C_5H_5^-$ subunit (toward the metal atom) and may play a role of a bridge for the charge-transfer.
2. The Li_3^+ and $C_5H_5^-$ ring in those structures can be considered as being σ-aromaticity and triple-fold aromaticity (π, σ_p, and σ_s), respectively.
3. Four important influencing factors to effect on the aromaticity of Li_3^+ ring are found. (a) The shape of structure (H- or T-shaped) obviously effects on the aromaticity of Li_3^+ ring because of the relative orientation between the Li_3^+ ring and OM subunit. (b) The existence of alkaline earth metal oxide evidently effects on the aromaticity of Li_3^+ ring. (c) The alkaline earth atomic number dependence of the aromaticity of Li_3^+ ring is found. (d) The end $C_5H_5^-$ subunit can increase the aromaticity of the end Li_3^+ ring.
4. Noticeably, in the H-shaped $Li_3OMC_5H_5$ (M = Be, Mg, and Ca), (a) the small-sized OM subunit near the Li_3^+ ring and the large-sized $C_5H_5^-$ subunit far from the Li_3^+ ring do not lead to the expected out-of-plane σ-aromaticity but increase the in-plane σ-aromaticity of Li_3^+ ring.
5. Owing to the low VIE, the H-shaped structure with diffusive electron cloud has electride characteristics, and the T-shaped structure with lithium anion has alkalide characteristics.

Those metal-[metal oxide]-nonmetal sandwich-like superalkali compounds are complex zwitterions and may be used as building blocks of material to construct the ionic crystals with supermolecule [14(a)] units.

References

1. (a) Gutsev, G. L.; Boldyrev, A. I. Chem Phys 1981, 56, 277; (b) Gutsev, G. L.; Boldyrev, A. I. Adv Chem Phys 1985, 61, 169; (c) Dudde, R.; Reihl, B. Chem Phys Lett 1982, 92, 262.
2. Bergeron, D. E.; Castleman, A. W.; Morisato, T.; Khanna, S. N. Science 2004, 304, 84.
3. (a) Bergeron, D. E.; Roach, P. J.; Castleman, A. W.; Jones, N. O.; Khanna, S. N. Science 2005, 307, 231; (b) Bergeron, D. E.; Castleman, A. W.; Morisato, T.; Khanna, S. N. J Chem Phys 2004, 121, 10456.
4. Li, X.; Kuznetsov, A. E.; Zhang, H. F.; Boldyrev, A. I.; Wang, L.-S. Science 2001, 291, 859.
5. (a) Kuznetsov, A. E.; Boldyrev, A. I.; Li, X.; Wang, L.-S. J Am Chem Soc 2001, 123, 8825; (b) Boldyrev, A. I.; Kuznetsov, A. E. Inorg Chem 2002, 41, 532; (c) Kuznetsov, A. E.; Boldyrev, A. I. Struct Chem 2002, 13, 141.
6. Zhan, C.-G.; Zheng, F.; Dixon, D. A. J Am Chem Soc 2002, 124, 14795.
7. (a) Kuznetsov, A. E.; Boldyrev, A. I.; Zhai, H.-J.; Li, X.; Wang, L.-S. J Am Chem Soc 2002, 124, 11791; (b) Alexandrova, A. N.; Boldyrev, A. I. J Phys Chem A 2003, 107, 554.
8. Byun, Y.-C.; Saebo, S.; Pittman, C. U., Jr. J Am Chem Soc 1991, 113, 3689.
9. (a) Li, Q. S.; Cheng, L. P. J Phys Chem A 2003, 107, 2882; (b) Lein, M.; Frunzke, J.; Timoshkin, A.; Frenking, G. Chem Eur J 2001, 7, 4155.
10. (a) Kealy, T. J.; Pauson, P. L. Nature 1951, 168, 1039; (b) Long, N. J. Metallocenes: An Introduction to Sandwich Complexes; Blackwell Science: Oxford, UK, 1998; (c) Urnezius, E.; Brennessel, W. W.; Cramer, C. J.; Ellis, J. E.; Schleyer, P. v. R. Science 2002, 295, 832.
11. (a) Mercero, J. M.; Ugalde, J. M. J Am Chem Soc 2004, 126, 3380; (b) Mercero, J. M.; Formoso, E.; Matxain, J. M.; Eriksson, L. A.; Ugalde, J. M. Chem Eur J 2006, 12, 4495; (c) Mercero, J. M.; Matxain, J. M.; Ugalde, J. M. Angew Chem Int Ed 2004, 43, 5485; (d) Fang, L.; Yang, G. C.; Qiu, Y. Q.; Su, Z. M. Theor Chem Acc 2008, 119, 329.
12. (a) Lein, M.; Frunzke, J.; Frenking, G. Angew Chem Int Ed 2003, 42, 1303; (b) Lein, M.; Frunzke, J.; Frenking, G. Angew Chem 2003, 115, 1341; (c) Roy, D. R.; Chattaraj, P. K. J Phys Chem A 2008, 112, 1612.
13. (a) Yang, L.-M.; Ding, Y.-H.; Sun, C.-C. ChemPhysChem 2006, 7, 2478; (b) Yang, L.-M.; Ding, Y.-H.; Sun, C.-C. Chem Eur J 2007, 13, 2546; (c) Yang, L.-M.; Ding, Y.-H.; Sun, C.-C. J Am Chem Soc 2007, 129, 658; (d) Yang, L.-M.; Ding, Y.-H.; Sun, C.-C. J Am Chem Soc 2007, 129, 1900; (e) Yang, L.-M.; Ding, Y.-H.; Sun, C.-C. J Phys Chem A 2007, 111, 10675.
14. (a) Sun, X.-Y.; Li, Z.-R.; Wu, D.; Sun, C.-C. Int J Quantum Chem 2007, 107, 1215; (b) Chen, W.; Li, Z.-R.; Wu, D.; Li, Y.; Sun, C.-C. J Chem Phys 2005, 123, 164306.
15. (a) Li, Z.-R.; Wang, F.-F.; Wu, D.; Li, Y.; Chen, W.; Sun, X.-Y.; Gu, F. L.; Aoki, Y. J Comput Chem 2006, 27, 986; (b) Li, Y.; Li, Z.-R.; Wu, D.; Chen, W.; Sun, C.-C. ChemPhysChem 2005, 6, 1; (c) Wang, F.-F.; Li, Z.-R.; Wu, D.; Sun, X.-Y.; Chen, W.; Li, Y.; Sun, C.-C. ChemPhysChem 2006, 7, 1136.
16. (a) Gagliardi, L.; Pyykkö, P. J Phys Chem A 2002, 106, 4690; (b) Yang, L.-M.; Wang, J.; Ding, Y.-H.; Sun, C.-C. J Phys Chem A 2007, 111, 9122.
17. Tsipis, A. C.; Chaviara, A. T. Inorg Chem 2004, 43, 1273.
18. Li, Q.-S.; Guan, J. J Phys Chem A 2003, 107, 8584.
19. (a) Dye, J. L. Science 2003, 301, 607; (b) Ichimura, A. S.; Dye, J. L.; Camblor, M. A.; Villaecusa, L. A. J Am Chem Soc 2002, 124, 1170; (c) Dye, J. L. Inorg Chem 1997, 36, 3816.
20. (a) Dye, J. L.; Ceraso, J. M.; Lok, M. T.; Barnett, B. L.; Tehan, F. J. J Am Chem Soc 1974, 96, 608; (b) Tehan, F. J.; Barnett, B. L.; Dye, J. L. J Am Chem Soc 1974, 96, 7203; (c) Dye, J. L. Chemtracts, Inorg Chem 1993, 5, 243; (d) Kim, J.; Ichimura, A. S.; Huang, R. H.; Redko, M.; Phillips, M.; Jackson, J. E.; Dye, J. L. J Am Chem Soc 1999, 121, 10666.
21. (a) Møller, C.; Plesset, M. S. Phys Rev 1934, 46, 618; (b) Head-Gordon, M.; Pople, J. A.; Frisch, M. J. Chem Phys Lett 1988, 153, 503.
22. Krishnan, R.; Binkley, J. S.; Seeger, R.; Pople, J. A. J Chem Phys 1980, 72, 650.
23. (a) Reed, A. E.; Weinstock, R. B.; Weinhold, F. J. J Chem Phys 1985, 83, 735; (b) Carpenter, J. E.; Weinhold, F. J Mol Struct 1988, 169, 41.
24. (a) Schleyer, P. v. R.; Maerker, C.; Dransfeld, A.; Jiao, H.; Hommes, N. J. V. E. J Am Chem Soc 1996, 118, 6317; (b) Schleyer, P. v. R.; Jiao, H. Pure Appl Chem 1996, 68, 209; (c) Schleyer, P. v. R.; Jiao, H.; Hommes, N. J. V. E.; Malkin, V. G.; Malkina, O. L. J Am Chem Soc 1997, 119, 12669; (d) Chen, Z.; Wannere, C. S.; Corminboeuf, C.; Puchta, R.; Schleyer, P. v. R. Chem Rev 2005, 105, 3842.
25. (a) Boldyrev, A. I.; Wang, L.-S. Chem Rev 2005, 105, 3716; (b) Goldfuss, B.; Schleyer, P. v. R.; Hampel, F. Organometallics 1996, 15, 1755; (c) Cyranski, M. K.; Krygowski, T. M.; Katritzky, A. L.; Schleyer, P. v. R. J Org Chem 2002, 67, 1333.
26. (a) Frisch, M. J.; Trucks, G. W.; Schlegel, H. B.; Scuseria, G. E.; Robb, M. A.; Cheeseman, J. R.; Montgomery, J. A.; Vreven, Jr., T.; Kudin, K. N.; Burant, J. C.; Millam, J. M.; Iyengar, S. S.; Tomasi, J.; Barone, V.; Mennucci, B.; Cossi, M.; Scalmani, G.; Rega, N.; Petersson, G. A.; Nakatsuji, H.; Hada, M.; Ehara, M.; Toyota, K.; Fukuda, R.; Hasegawa, J.; Ishida, M.; Nakajima, T.; Honda, Y.; Kitao, O.; Nakai, H.; Klene, M.; Li, X.; Knox, J. E.; Hratchian, H. P.; Cross, J. B.; Bakken, V.; Adamo, C.; Jaramillo, J.; Gomperts, R.; Stratmann, R. E.; Yazyev, O.; Austin, A. J.; Cammi, R.; Pomelli, C.; Ochterski, J. W.; Ayala, P. Y.; Morokuma, K.; Voth, G. A.; Salvador, P.; Dannenberg, J. J.; Zakrzewski, V. G.; Dapprich, S.; Daniels, A. D.; Strain, M. C.; Farkas, O.; Malick, D. K.; Rabuck, A. D.; Raghavachari, K.; Foresman, J. B.; Ortiz, J. V.; Cui, Q.; Baboul, A. G.; Clifford, S.; Cioslowski, J.; Stefanov, B. B.; Liu, G.; Liashenko, A.; Piskorz, P.; Komaromi, I.; Martin, R. L.; Fox, D. J.; Keith, T.; Al-Laham, M. A.; Peng, C. Y.; Nanayakkara, A.; Challacombe, M.; Gill, P. M. W.; Johnson, B.; Chen, W.; Wong, M. W.; Gonzalez, C.; Pople, J. A. Gaussian 03, Revision B.03; Gaussian, Inc.: Pittsburgh, PA, 2003; (b) Dennington, R., II; Todd, K.; Millam, J.; Eppinnett, K.; Hovell, W. L.; Gilliland, R. GaussView, Version 3.09; Semichem, Inc.: Shawnee Mission, KS, 2003.
27. Lide, D. R. CRC Handbook of Chemistry and Physics; CRC Press: Boca Raton, 2000.
28. (a) Corminboeuf, C.; Heine, T.; Seifert, G.; Schleyer, P. v. R. Phys Chem Chem Phys 2004, 6, 273; (b) Schleyer, P. v. R.; Manoharan, M.; Wang, Z.; Kiran, X. B.; Jiao, H.; Puchta, R.; Hommes, N. J. R. V. E. Org Lett 2001, 3, 2465; (c) Zhai, H. J.; Wang, L.-S.; Kuznetsov, A. E.; Boldyrev, A. I. J Phys Chem A 2002, 106, 5600.
29. (a) Zubarev, D. Y.; Boldyrev, A. I. Phys Chem Chem Phys 2008, 10, 5207; (b)Zubarev, D. Y.; Boldyrev, A. I. J Org Chem 2008, 73, 9521.